2015

Theoretical Examination of Solvent and R Group Dependence in Gold Thiolate Nanoparticle Synthesis

Suzanne M. Neidhart

Brian M. Barngrover
Stephen F Austin State University, barngrovbm@sfasu.edu

Christine M. Aikens

Theoretical examination of solvent and R group dependence in gold thiolate nanoparticle synthesis

Suzanne M. Neidhart , Brian M. Barngrover and Christine M. Aikens *

Department of Chemistry, Kansas State University, Manhattan, KS 66506, USA. E-mail: cmaikens@ksu.edu

Received 24th September 2014 **, Accepted 9th February 2015**

First published on the web 9th February 2015

The growth of gold thiolate nanoparticles can be affected by the solvent and the R group on the ligand. In this work, the difference between methanol and benzene solvents as well as the effect of alkyl (methyl) and aromatic (phenyl) thiols on the reaction energies and barrier heights is investigated theoretically. Density functional theory (DFT) calculations using the BP86 functional and a triple ζ polarized basis set show that the overall reaction favors methylthiol over phenylthiol with reaction energies of −0.54 and −0.39 eV in methanol, respectively. At the same level of theory, the methanol solvent is favored over the benzene solvent for reactions forming ions; in benzene, the overall reaction energies for methylthiol and phenylthiol reacting with $AuCl_4^-$ to form $Au(HSR)_2^+$ are 0.37 eV and 0.44 eV, respectively. Methylthiol in methanol also has the lowest barrier heights at about 0.3 eV, whereas phenylthiol has barrier heights around 0.4 eV. Barrier heights in benzene are significantly larger than those in methanol.

Introduction

Gold thiolate nanoparticles can be utilized in a number of applications, such as catalysis,[1] the treatment of cancer,[2] DNA tagging,[3,4] solar cells,[5] and water purification.[6] Certain morphologies are ideal for different applications. Gold nanorods have a particular plasmon resonance depending on their aspect ratio and this can be particularly useful in the treatment of cancer.[7] In

contrast, small gold nanospheres are commonly utilized in catalysis due to their affinity to bind oxygen.[8] Nanostars of gold are becoming promising structures for solar cell technology due to the high ratio of energy converted to power.[5] An understanding of the growth mechanisms of these systems will lead to better control over the formation of particular morphologies.

The most well-known gold thiolate complexes are the 'magic clusters'.[9] The most famous clusters are $Au_{25}(SR)_{18}^-$,[10–12] $Au_{38}(SR)_{24}$,[13,14] $Au_{102}(SR)_{44}$,[15] and $Au_{144}(SR)_{60}$,[16] although other stoichiometries have also been observed, such as $Au_{36}(SR)_{24}$[17,18] and $Au_{99}(SR)_{42}$.[19] Aliphatic ligands have typically been used in the synthesis of $Au_{25}(SR)_{18}^-$, $Au_{38}(SR)_{24}$, and $Au_{144}(SR)_{60}$, whereas aromatic ligands have been employed in the synthesis of $Au_{36}(SR)_{24}$, $Au_{99}(SR)_{42}$, $Au_{102}(SR)_{44}$, and other systems.[17–22] Thus, the choice of ligand appears to affect the stoichiometry of the final product. The ligands, which coat the exterior of the molecule, are made up of Au_mSR_n subunits that protect the gold core.

Gold thiolate nanoparticles are often synthesized by the Brust–Schiffrin (B–S) method[23] or variations of this method.[24] The B–S method is a two solvent phase reduction of tetrachloroaurate ($AuCl_4^-$) using sodium borohydride ($NaBH_4$) with a thiol (HSR), in a one-to-ten-to-four ratio, which results in 1–3 nm gold particles. In one of the variations of the method, Yee *et al.* recognized that the two-phase method did not fit well for ω-substituted thiols due to the difficulty in purification of the product and thus looked into a one-phase method.[25] They used tetrahydrofuran (THF) because it does not have solubility issues with ω-substituted thiols unlike the two-phase system. A phase-transfer reagent was not required in the single-phase method unlike the two-phase method. Even though the starting materials are the same, both syntheses yielded different particles sizes; the single-phase particles are approximately 2.5 nm in diameter and the two-phase particles are 2.1 nm. Sun *et al.* demonstrated that when synthesizing decanethiolate gold nanoparticles in single- and two-phase approaches, the dimensions of the particles and thiol grafting density are different, which is in agreement with Yee *et al.*[26]

In another modification to the original B–S synthesis, Goulet *et al.* observed that a two-to-one ratio of the thiol ligand and Au(III) is enough to cause reduction of Au(III) to Au(I) and form a disulfide.[24] Barngrover and Aikens performed density functional theory (DFT) calculations and also found that the two-to-one ratio is enough to cause reduction of Au(III).[27]

We modeled the one-phase method with a four-to-one ratio of phenyl thiol ligand to gold salt in methanol and benzene. The aromatic ligand is of interest to compare with aliphatic thiol

ligands that were previously studied by our group.[27] Pathway B from the previous body of work, which was the most thermodynamically stable pathway found, is the pathway we modeled in this study; this pathway involves the reduction of Au(III) to Au(I) by two equivalents of thiol ligand and the subsequent reaction with two more thiol ligands.

Computational details

The Amsterdam Density Functional (ADF)[28] program was used to find the reaction energies and transition states. All the geometries were visualized using MacMolPlt version 7.4.4 and figure images were created using Jmol version 13.0.14.[29,30] The chemical structures were optimized using the Becke–Perdew (BP86)[31,32] functional and a triple-ζ with polarization functions (TZP) basis set. Scalar relativistic effects were accounted for using the Zero Order Regular Approximation (ZORA).[33] Solvation was taken into account through the Conductor-like Screening Model (COSMO), which represents the solvent by its dielectric constant.[34–37]

All calculations in this work have the phenyl group on the thiol ligand unless stated otherwise. Intermediates and transition states reported are fully optimized. Hessian calculations were performed analytically for the transition states. All transition states have an imaginary frequency corresponding to the expected nuclear motion. In the second and fourth transition states in methanol and benzene, a second imaginary frequency with zero intensity and a value <20i cm^{-1} was obtained. The energies reported in this work include zero-point energy corrections.

Results and discussion

First thiol reaction

We investigated the overall pathway in a step-wise addition of four phenylthiols to gold(III) chloride as shown in Scheme 1. The pathway was calculated in both methanol and benzene solvents. The first addition of a thiol to the gold complex proceeds through a bipyramidal transition state with a barrier height of 0.42 eV in methanol (Fig. 1) and 0.66 eV in benzene (Fig. 2) and then a chloride ion is expelled. The chloride ion then reacts with the hydrogen on the sulfur atom and detaches a proton to produce HCl. The thiol attaching to the gold(III) and the

subsequent discharging of a chloride ion, reaction (1A), has a reaction energy of 0.16 eV in methanol (Fig. 1). The proton transfer, denoted (1A′) in Scheme 1, from the thiol to the chloride ion in methanol has an energy of −0.26 eV for an overall reaction energy of −0.10 eV (Fig. 1 and Table 1). For comparison, we have also performed these calculations in benzene. In benzene, reaction (1A) yields an energy of 0.49 eV and a reaction (1A′) yields an energy of −0.51 eV. The overall reaction in benzene produces an energy of −0.02 eV (Fig. 2 and Table 1). The chloride ion is more favored to form in the methanol solvent than the benzene solvent, since the polar solvent can more easily stabilize the negative ion. The initial chloride removal may not occur in a nonpolar solvent.

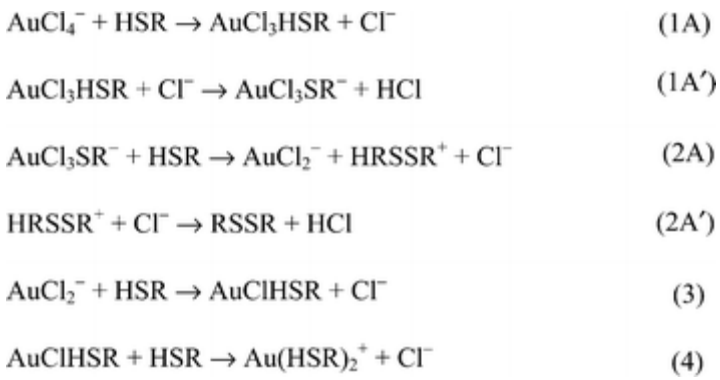

Scheme 1

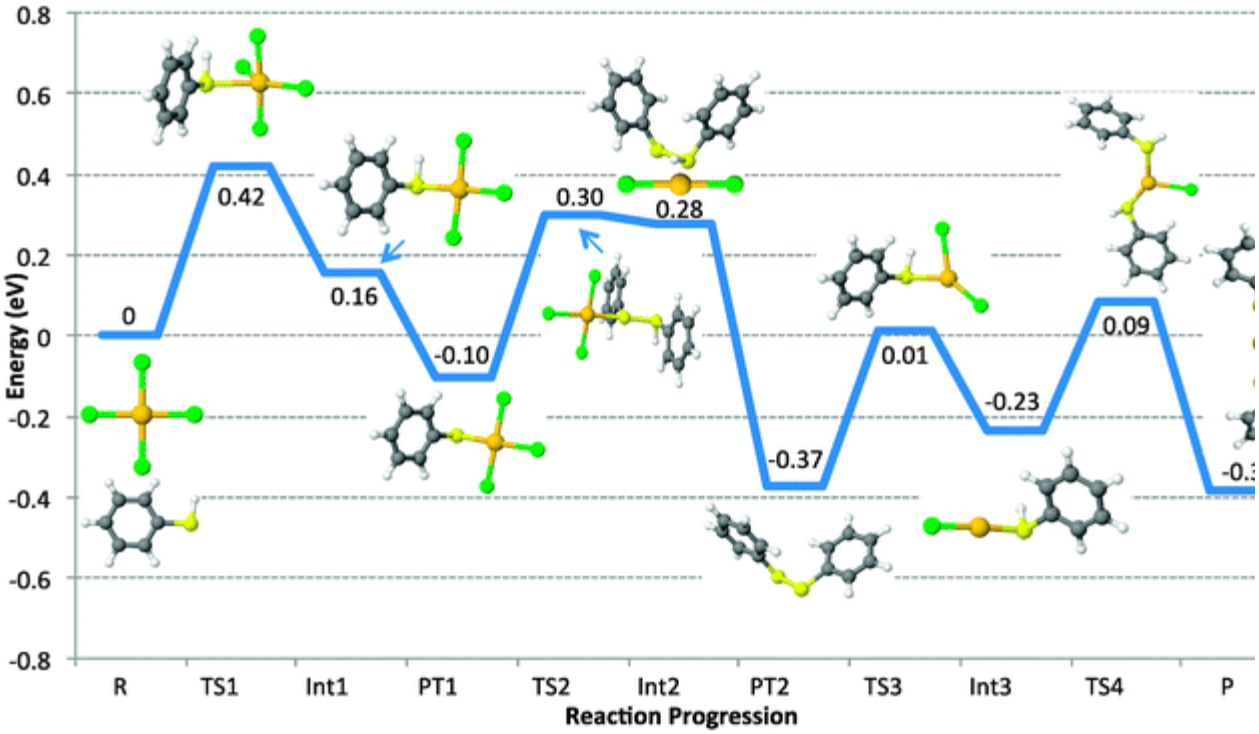

Fig. 1 Overall reaction involving addition of four equivalents of phenylthiol to $AuCl_4^-$ in methanol. Gold = gold, chloride = green, carbon = gray, sulfur = yellow, and hydrogen = white. R = reactants, TS = transition state, Int = intermediate, PT = proton transfer, and P = products. HCl and Cl^- are not shown for clarity.

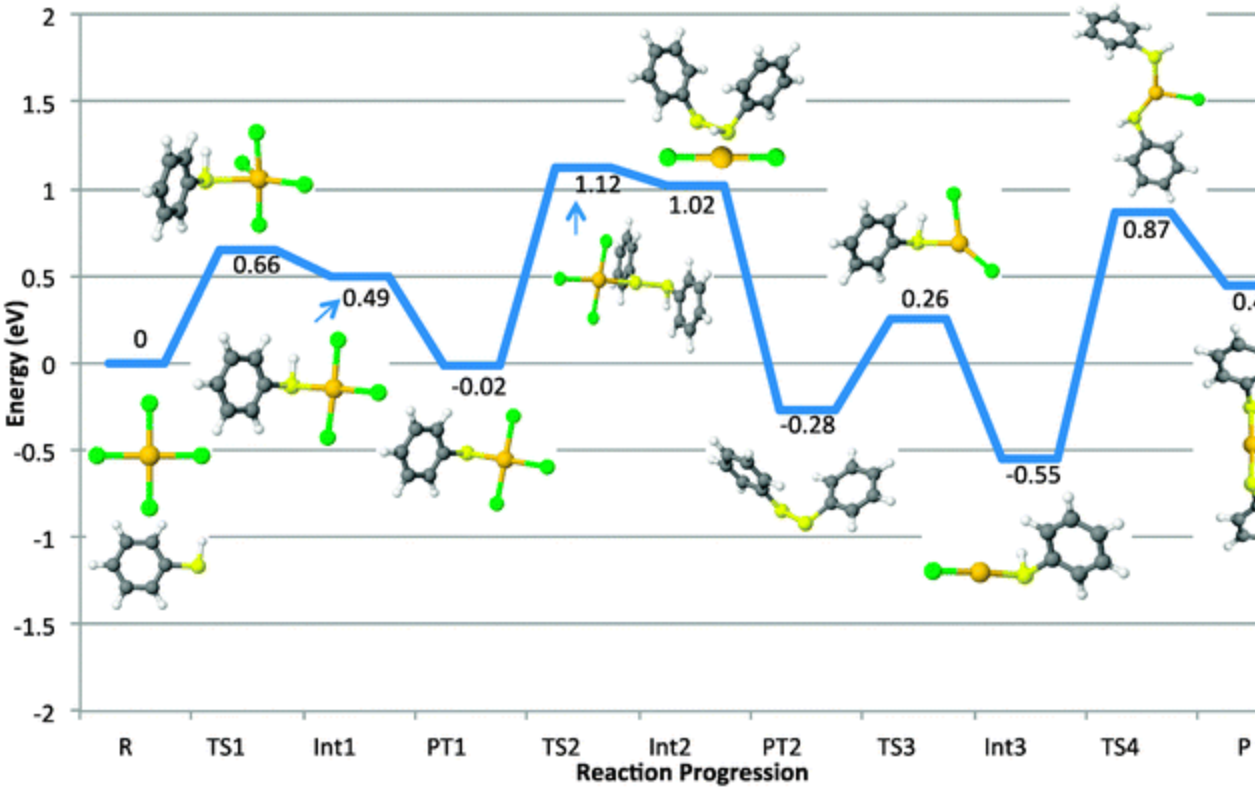

Fig. 2 Overall reaction involving addition of four equivalents of phenylthiol to $AuCl_4^-$ in benzene. Gold = gold, chloride = green, carbon = gray, sulfur = yellow, and hydrogen = white. R = reactants, TS = transition state, Int = intermediate, PT = proton transfer, and P = products. HCl and Cl^- are not shown for clarity.

Table 1 Comparison of reactions in methanol and benzene and with methyl and phenyl thiol. R = methyl values in methanol are from ref. 27

	Methanol		**Benzene**	
Solvent	**R = methyl**[27]	**R = phenyl**	**R = methyl**	**R = phenyl**
Overall reaction energy (eV)	−0.54	−0.39	0.37	0.44
Reaction (1) (eV)	−0.17	−0.10	−0.10	−0.02
Reaction (2) (eV)	−0.41	−0.27	−0.35	−0.26
Reaction (3) (eV)	−0.10	0.14	0.58	−0.27

Reaction (4) (eV)	0.14	−0.16	0.24	0.99

Second thiol reaction

The second addition of thiol reacts with the monosubstituted gold complex to form a disulfide. The initial reaction (2A) results in a reaction energy of 0.38 eV and a barrier height of 0.40 eV in methanol (Fig. 1). There are three structures that are produced from the initial reaction: $AuCl_2^-$, Cl^-, and $H(Ph)SSPh^+$. The second part (2A′) of the reaction is the proton transfer from the protonated disulfide to the chloride ion, resulting in a neutral disulfide and HCl. This step is similar to the proton dissociation in the first addition of a thiol, and has an energy of −0.65 eV. Overall, the reaction in methanol has a calculated reaction energy of −0.27 eV.

In benzene the overall reaction is favorable, though under closer examination it appears unlikely with a barrier height of 1.14 eV. Reaction (2A) has a calculated reaction energy of 1.04 eV and reaction (2A′) has an energy of −1.30 eV for an overall energy of −0.26 eV (Table 1). The charge separation in the nonpolar solvent is highly unfavorable, causing the initial thiol-for-chloride substitution to be highly endothermic and the subsequent proton removal by the chloride to form neutral HCl to be highly exothermic.

Third thiol reaction

The third thiol reacts with the $AuCl_2^-$ species to eject a chloride and form a monosubstituted gold(I) complex. In methanol, the reaction energy was calculated to be 0.14 eV with a barrier height of 0.38 eV, so it is slightly endothermic. In benzene, the reaction energy was calculated to be −0.27 eV with a barrier height of 0.54 eV (Table 1).

Recent work by Zhang *et al.* has suggested that the chloride does not fully dissociate in nonpolar solvents.[38] We find that the chloride ion is not favored in either methanol or benzene solvents to cause a subsequent proton transfer and yield HCl; rather, if generated in the reaction, the chloride remains in the ionic form. As discussed previously by Barngrover and Aikens,[27] removal of the chloride and proton are required for potential formation of $(AuSR)_n$ polymers.

Fourth thiol reaction

The fourth addition of the thiol acts on a monosubstituted gold complex and causes the last chloride ligand to be removed and another gold–sulfur bond to form. The barrier height for the reaction is calculated to be 0.32 eV with a reaction energy of −0.16 eV (Fig. 1) in methanol. In benzene the reaction energy is 0.99 eV (Fig. 2) with a barrier height of 1.42 eV. Again, the formation of a charged species in nonpolar solvent is highly unfavored compared to reaction in the more polar methanol solvent.

The overall reaction energies in methanol and benzene were calculated to be −0.39 eV and 0.44 eV, respectively. The reaction could reasonably occur in methanol and the first two steps would be the driving force for the third and fourth step to occur. This pathway is unreasonable in the benzene solvent without considering the effects of counterions. The charge separation in the second reaction causes a highly endothermic reaction in benzene and cannot be reasonably overcome.

R group dependence

In addition to the solvent dependence of the reaction energies for R = Ph, we can also examine the influence of the R group on the reaction energies in both methanol and benzene. Our current work can be compared to prior work where the R group is a methyl and the solvent is methanol.[27] Reaction (1) ((1A) followed by (1A′)) is more favored with the methyl group, since this yields a reaction energy of −0.17 eV whereas the phenyl group has a reaction energy of −0.10 eV (Table 1). Reaction (2) ((2A) and (2A′)) is more favorable with the methyl ligand with a reaction energy of −0.41 eV; the phenyl ligand has a reaction energy of −0.27 eV. The third reaction is also more favored with the methyl ligand than the phenyl ligand. The reaction energy for methyl in reaction (3) is calculated to be −0.10 eV and for phenyl it is 0.14 eV. The reaction energy for reaction (4) is more favored with phenyl and is calculated to be −0.16 eV and for methyl the reaction energy is 0.14 eV. This may possibly explain why most experimental syntheses employ aliphatic rather than aromatic ligands. In addition, we have examined the reactions of both methylthiol and phenylthiol in benzene. Most of the steps are more favorable (less endothermic or more exothermic) for methylthiol than phenylthiol (Table 1); however, they are not as favored as the

reactions carried out in methanol.

Conclusions

The synthesis of gold thiolate nanoclusters or nanoparticles through the Brust–Schiffrin method has been performed for years with minor understanding of the mechanism for the formation. This work is centered on the modified single-phase Brust–Schiffrin method utilizing two different solvents. Our calculations are performed with a four-to-one ratio of phenylthiol to gold salt and showed that the reduction of gold(III) to gold(I) and formation of a disulfide is favorable in methanol solvent. Compared to previous work done with the same pathway, it can be concluded that the addition of phenylthiol ligands to the gold salt is less thermodynamically favorable than the addition of methylthiol groups. The reduction of gold(III) to gold(I) and the formation of a disulfide in benzene is thermodynamically less favorable. Charge separation in benzene is substantially higher in energy than in methanol. Since this reaction is traditionally conducted in toluene, which is nonpolar similar to benzene, a different pathway must be explored to explain the growth in nonpolar solvents.

Acknowledgements

We would like to thank the K-State REU Program, which is cofunded by the ASSURE program of the Department of Defense in partnership with the National Science Foundation REU Site program under Grant number 1004991. The National Science Foundation under Grant number CHE-1213771 also supported this work.

References

1. H. Sakurai, K. Koga, Y. Iizuka and M. Kiuchi, *Appl. Catal., A*, 2013, **462–463**, 236–246 CrossRef CAS PubMed.
2. M. A. Mackey, F. Saira, M. A. Mahmoud and M. A. El-Sayed, *Bioconjugate Chem.*, 2013, **24**, 897–906 CrossRef CAS PubMed.
3. X. Fu, R. Huang, J. Wang and B. Chang, *RSC Adv.*, 2013, **3**, 13451 RSC.

4. Y. Akhlaghi, M. Kompany-Zareh and M. R. Hormozi-Nezhad, *Anal. Chem.*, 2012, **84**, 6603–6610 CrossRef CAS PubMed.
5. D. Kozanoglu, D. H. Apaydin, A. Cirpan and E. N. Esenturk, *Org. Electron.*, 2013, **14**, 1720–1727 CrossRef CAS PubMed.
6. H. Qian, L. A. Pretzer, J. C. Velazquez, Z. Zhao and M. S. Wong, *J. Chem. Technol. Biotechnol.*, 2013, **88**, 735–741 CrossRef CAS.
7. S. Link and M. A. El-Sayed, *J. Phys. Chem. B*, 1999, **103**, 8410–8426 CrossRef CAS.
8. M. Turner, V. B. Golovko, O. P. H. Vaughan, P. Abdulkin, A. Berenguer-Murcia, M. S. Tikhov, B. F. G. Johnson and R. M. Lambert, *Nature*, 2008, **454**, 981–983 CrossRef CAS PubMed.
9. M. Walter, J. Akola, O. Lopez-Acevedo, P. D. Jadzinsky, G. Calero, C. J. Ackerson, R. L. Whetten, H. Grönbeck and H. Häkkinen, *Proc. Natl. Acad. Sci. U. S. A.*, 2008, **105**, 9157–9162 CrossRef CAS PubMed.
10. M. Zhu, C. M. Aikens, F. J. Hollander, G. C. Schatz and R. Jin, *J. Am. Chem. Soc.*, 2008, **130**, 5883–5885 CrossRef CAS PubMed.
11. J. Akola, M. Walter, R. L. Whetten, H. Häkkinen and H. Grönbeck, *J. Am. Chem. Soc.*, 2008, **130**, 3756–3757 CrossRef CAS PubMed.
12. M. W. Heaven, A. Dass, P. S. White, K. M. Holt and R. W. Murray, *J. Am. Chem. Soc.*, 2008, **130**, 3754–3755 CrossRef CAS PubMed.
13. O. Lopez-Acevedo, H. Tsunoyama, T. Tsukuda, H. Häkkinen and C. M. Aikens, *J. Am. Chem. Soc.*, 2010, **132**, 8210–8218 CrossRef CAS PubMed.
14. H. Qian, W. T. Eckenhoff, Y. Zhu, T. Pintauer and R. Jin, *J. Am. Chem. Soc.*, 2010, **132**, 8280–8281 CrossRef CAS PubMed.
15. P. D. Jadzinsky, G. Calero, C. J. Ackerson, D. A. Bushnell and R. D. Kornberg, *Science*, 2007, **318**, 430–433 CrossRef CAS PubMed.
16. O. Lopez-Acevedo, J. Akola, R. L. Whetten, H. Grönbeck and H. Häkkinen, *J. Phys. Chem. C*, 2009, **113**, 5035–5038 CAS.
17. P. R. Nimmala and A. Dass, *J. Am. Chem. Soc.*, 2011, **133**, 9175–9177 CrossRef CAS PubMed.

18. C. Zeng, H. Qian, T. Li, G. Li, N. L. Rosi, B. Yoon, R. N. Barnett, R. L. Whetten, U. Landman and R. Jin, *Angew. Chem., Int. Ed.*, 2012, **124**, 13291–13295 CrossRef.
19. G. Li, C. Zeng and R. Jin, *J. Am. Chem. Soc.*, 2014, **136**, 3673–3679 CrossRef CAS PubMed.
20. R. C. Price and R. L. Whetten, *J. Am. Chem. Soc.*, 2005, **127**, 13750–13751 CrossRef CAS PubMed.
21. P. R. Nimmala and A. Dass, *J. Am. Chem. Soc.*, 2011, **133**, 9175–9177 CrossRef CAS PubMed.
22. C. Zeng, C. Liu, Y. Pei and R. Jin, *ACS Nano*, 2013, **7**, 6138–6145 CrossRef CAS PubMed.
23. M. Brust, M. Walker, D. Bethell, D. J. Schiffrin and R. Whyman, *J. Chem. Soc., Chem. Commun.*, 1994, 801–802 RSC.
24. P. J. G. Goulet and R. B. Lennox, *J. Am. Chem. Soc.*, 2010, **132**, 9582–9584 CrossRef CAS PubMed.
25. C. K. Yee, R. Jordan, A. Ulman, H. White, A. King, M. Rafailovich and J. Sokolov, *Langmuir*, 1999, **15**, 3486–3491 CrossRef CAS.
26. Y. Sun, A. I. Frenkel, H. White, L. Zhang, Y. Zhu, H. Xu, J. C. Yang, T. Koga, V. Zaitsev, M. H. Rafailovich and J. C. Sokolov, *J. Phys. Chem. B*, 2006, **110**, 23022–23030 CrossRef CAS PubMed.
27. B. M. Barngrover and C. M. Aikens, *J. Am. Chem. Soc.*, 2012, **134**, 12590–12595 CrossRef CAS PubMed.
28. G. te Velde, F. M. Bickelhaupt, E. J. Baerends, C. Fonseca Guerra, S. J. A. van Gisbergen, J. G. Snijders and T. Ziegler, *J. Comput. Chem.*, 2001, **22**, 931–967 CrossRef CAS.
29. B. M. Bode and M. S. Gordon, *J. Mol. Graphics Modell.*, 1998, **16**, 133–138 CrossRef CAS.
30. Jmol: an open-source Java viewer for chemical structures in 3D. http://www.jmol.org/.
31. J. P. Perdew, *Phys. Rev. B: Condens. Matter Mater. Phys.*, 1986, **34**, 7406 CrossRef.
32. A. D. Becke, *Phys. Rev. A: At., Mol., Opt. Phys.*, 1988, **38**, 3098–3100 CrossRef CAS.

33. E. van Lenthe, A. Ehlers and E.-J. Baerends, *J. Chem. Phys.*, 1999, **110**, 8943–8953 CrossRef CAS PubMed.
34. C. C. Pye and T. Ziegler, *Theor. Chem. Acc.*, 1999, **101**, 396–408 CrossRef CAS.
35. A. Klamt and G. Schuurmann, *J. Chem. Soc., Perkin Trans. 2*, 1993, 799–805 RSC.
36. A. Klamt, *J. Phys. Chem.*, 1995, **99**, 2224–2235 CrossRef CAS.
37. A. Klamt and V. Jonas, *J. Chem. Phys.*, 1996, **105**, 9972–9981 CrossRef CAS PubMed.
38. X.-N. Zhang, R. Wang and G. Xue, *Chin. Phys. B*, 2014, **23**, 098201 CrossRef.